Available online at www.sciencedirect.com
SCIENCE DIRECT®
Geomorphology 51 (2003) 175–185
GEOMORPHOLOGY
www.elsevier.com/locate/geomorph

Field measurements of drag coefficients for model large woody debris

Bretagne Hygelund[a], Michael Manga[b,*]

[a] Department of Geological Sciences, University of Oregon, Eugene, OR 97403, USA
[b] Department of Earth and Planetary Science, University of California, Berkeley, CA 94720, USA

Received 29 June 2001; received in revised form 22 September 2001; accepted 18 October 2002

Abstract

Woody debris in rivers can be a significant source of roughness and consequently influences flow at both the local and reach scale. In order to develop a better quantitative understanding of the interaction between wood in rivers and stream flow, we thus performed a set of field measurements of the drag on model woody debris for conditions that prevail in typical natural streams. Our model debris consisted of PVC "logs" with diameters between 4 and 30 cm. The field setting allowed us to consider the hydrodynamic influence of a rough stream bottom, and our measurements thus complement previously published flume-based measurements. We found that, owing to the variation of velocity with water depth, some of our results differed appreciably from measurements made in smooth flumes. We determined the effects of (i) the orientation of the log, (ii) the size of the log relative to the water depth, (iii) the depth of the log in the water column, and (iv) leafless branches on the log. We found that the orientation of the log had no significant effect on the apparent drag coefficient. By contrast, because the water velocity varies with depth, the position of the log in the water column influenced the apparent drag for small logs. For large logs (diameter >30% of the water depth), however, the position of the log had little effect on drag. The ratio of the diameter of the log to the water depth, a quantity called "blockage," also affected drag. As blockage increased, drag increases. For blockages greater than about 0.3, however, the drag becomes independent of blockage. Finally, we found that the presence of leafless branches does not increase the drag (within measurement sensitivity).

Keywords: Large woody debris; Drag coefficients; Flow resistance; Stress partitioning

1. Introduction

Woody debris in rivers can be an important source of flow resistance and as a result will influence channel properties and morphology at both the local and reach scale (e.g., Lisle, 1995; Dudley et al., 1998). At the local scale, woody debris can create its own set of geomorphic features such as pools and bars (e.g., Bisson et al., 1987; Robison and Beschta, 1990). At the reach scale, when wood is added to a river, the increase in flow resistance can inhibit the stream's ability to transport sediment (e.g., Assani and Petit, 1995; Buffington and Montgomery, 1999) and may thus increase sediment storage (e.g., Smith et al., 1993). However, because woody debris diverts the flow of water, locally it will increase stream velocity.

* Corresponding author.
E-mail address: manga@seismo.berkeley.edu (M. Manga).

0169-555X/02/$ - see front matter © 2002 Elsevier Science B.V. All rights reserved.
PII: S0169-555X(02)00335-5

Consequently, sediment transport may be promoted locally and may result in bank erosion (e.g., Nakamura and Swanson, 1993; Trimble, 1997). Woody debris can therefore affect properties and dynamics at the reach scale, such as the width to depth ratio of stream channels (Bilby and Ward, 1991; Whiting and Moog, 2001) and channel stability (Bilby, 1983).

The effects of woody debris on stream flow depend on both hydraulic conditions in the river and geometric characteristics of the wood, such as spacing of debris and the size of debris relative to water depth (e.g., Gippel et al., 1996). Field studies have shown that the length and diameter of deposited pieces of wood increase with increasing stream discharge (e.g., Piegay and Gurnell, 1997). Moreover, the length, diameter, and volume of wood increase with increasing stream width (Bilby and Ward, 1991; Abbe and Montgomery, 1996). Such field observations, combined with flume experiments and models of wood movement (e.g., Braudrick et al., 1997), suggest that the behavior of wood in rivers can be quantified from knowledge of channel geometry, wood characteristics, and prevailing hydraulic conditions (Braudrick and Grant, 2000). An understanding of wood dynamics, coupled with an understanding of the geomorphic effects of wood, would provide a framework for better interpreting and predicting the response of fluvial systems to changes in wood loading (Manga and Kirchner, 2000).

One convenient and useful measure of the hydraulic impact of large woody debris (logs) in the fluvial system is the drag force, the force that flowing water exerts on a log. Gippel et al. (1996) measured the drag force on model woody debris in a laboratory flume. The drag force was determined as a function of hydraulic conditions (water velocity and water depth) and geometric properties of the logs (log diameter, shape, depth, and orientation). Our goal in the present complementary study is to use direct field measurements to provide improved constraints on the hydraulic effects of logs for conditions that prevail in natural streams. Owing to the rough bottom of natural streams, water velocity varies with depth and we will see that the variation of water velocity can have a significant effect on the drag force. Despite the geometric and hydrodynamic limitations inherent in our field study, measurements such as those presented here combined with flume measurements provide a starting point for quantitative prediction of the interaction between wood and stream flow, entrainment of wood, and stress partitioning by woody debris.

2. Drag on wood

When a solid object is submerged in a moving body of fluid, a downstream force will be exerted on the object. In this study, we are interested in the downstream force exerted on a log (circular cylinder) in a river. The downstream force on the submerged log will be

$$F_{\mathrm{d}} = \frac{1}{2}\rho C_{\mathrm{D}}^{\mathrm{app}} \bar{u}^2 A \sin\theta \tag{1}$$

where F_{d} is the downstream force, ρ is the density of water, A is the submerged cross-sectional area of the log, θ is the angle of the log relative to downstream, $\bar{u}$ is the depth-averaged velocity of the water as it approaches the log, and $C_{\mathrm{D}}^{\mathrm{app}}$ is a dimensionless constant of proportionality called the apparent drag coefficient. $C_{\mathrm{D}}^{\mathrm{app}}$ is an apparent drag coefficient (thus the superscript ^{app}) because it is measured for the given set of geometric and hydraulic conditions. The application of classical values for the steady motion of circular cylinders in infinitely large volumes of fluid, such as those that can be found in most fluid mechanics texts (e.g., Batchelor, 1967), may not be quantitatively valid in natural streams for several reasons: stream flow is not steady, velocity varies with depth in the water column, a free surface can interact with the flow and the log, the water column has a finite depth, and logs are "rough." Indeed, we will see by comparing our measurements with the flume measurements of Gippel et al. (1996) that the rough stream bottom can have a significant influence on $C_{\mathrm{D}}^{\mathrm{app}}$.

In this study, we directly measure $C_{\mathrm{D}}^{\mathrm{app}}$ in natural streams while varying the geometric and hydraulic conditions. The hydraulic conditions include the Reynolds number ($Re = \bar{u}d/\nu$), where d is the diameter of the log below the water surface and ν is the kinematic viscosity of water, and the Froude number ($Fr = \bar{u}/\sqrt{g\bar{z}}$), where g is gravitational acceleration and $\bar{z}$ is the mean water depth. Unfortunately, Re and Fr cannot both be scaled independently. Flumes and model wood are both usually smaller than in the field setting, which requires $\bar{u}$ to be greater than in the field

setting in order to scale *Re*. Nevertheless, both here and in the flume experiments of Gippel et al. (1996), *Fr* is quite a bit less than 1 so that the measurements should be directly comparable.

In order to keep the measurements practical and the interpretation of the results straightforward, we focus on single logs. We thus ignore the interactions between individual logs. Previous studies have shown that the hydraulic interactions between logs can be non-negligible when they are separated by as much as 10 log diameters (e.g., Ranga Raju et al., 1983). We also ignore the contribution to flow resistance provided by bedforms that may be created by woody debris.

3. Methods

3.1. Measurement locality

Measurements were made in the Fall and Quinn Rivers, two spring-dominated streams located in the Cascade Mountains of central Oregon. Spring-dominated rivers provide a convenient setting for our study because they have uniform flow and are generally shallow and flat-bottomed (Whiting and Stamm, 1995; Manga, 1997).

In selecting a measurement area, we located a straight section in each river where the water depth in the measurement area was approximately constant (to within 2 cm). We also required that no obstructions affected the water flow, such as stream vegetation or woody debris. Within this channel cross-section, we chose a 2-m subregion over which the water velocity was approximately constant. We measured the water velocity with a Price pygmy current meter. The size of the bed material was determined by dry sieving between 1 and 2 kg of the bed surface material, and analyses of the diameter (d_{50} and d_{90} in mm) for the 50th and 90th percentile size ranges indicate that both rivers are gravel-bedded. Table 1 summarizes the characteristics of measurement reaches.

3.2. Measurement apparatus

To gain an understanding of how the drag coefficient varies with geometric properties, we built an apparatus that measures torque on logs of various sizes at different depths and orientations. We were also able to vary the shape of the log in order to simulate the effect of branches. For each set of measurements, we related torque to the drag force and calculated C_D^{app}.

Table 1
Characteristics of the Fall and Quinn rivers

Name	$\bar{u}$ (m/s)	$\bar{z}$ (cm)	Temperature (°C)	d_{90} (mm)	d_{50} (mm)	*Fr*
Quinn River	0.16	40	4.4	4.0	3.5	0.082
Fall River	0.33	48	6.5	20.0	16.0	0.15

In order to measure torque, we attached seven PVC pipes (model logs) one at a time to a freely rotating pole that was fixed to a footplate (Fig. 1). Each log was filled with enough Styrofoam to make it neutrally buoyant in water. We then used two Proto dial torque wrenches, with torque ranges between 0.0 and 9.0 and 0.0 and 70.0 N m, to measure the torque required to hold the log in place at any given orientation. Uncertainties for these two torque wrenches are 0.1 and 1 N m, respectively. Orientations were measured using a Brunton compass. The attachment between the log and the pole was vertically adjustable, allowing us to measure torque at any given depth and orientation. All of the logs were 1.8 m in length, and the diameters varied (48.5, 60.5, 101, 114, 168, 221, and 274 mm). Measurements were repeatable and user-independent. We also varied a blockage ratio, the fraction of the water depth blocked by the log, where blockage values ranged between 0.1 and 0.7. *Re* ranged between 4×10^3 and 6×10^4, and *Fr* was <0.2 (Table 1). This range of *Re* is typical of conditions that prevail in both lowland rivers and headwater streams. The upper limit, however, is lower than *Re* that can be reached at bankfull stage. For *Re* about one order of magnitude greater than the studied *Re*, the boundary layer around the log becomes fully turbulent and C_D^{app} is reduced by a factor of about 3 (e.g., Batchelor, 1967). The upper limit of *Re* that we were able to study was limited by the physical strength of the authors.

3.3. The relationship between torque and drag

When a log of length L is submerged in water, the downstream force F_d relates to torque by the expression

$$F_d = \frac{2T}{\sin\theta(2\gamma + L)}, \quad (2)$$

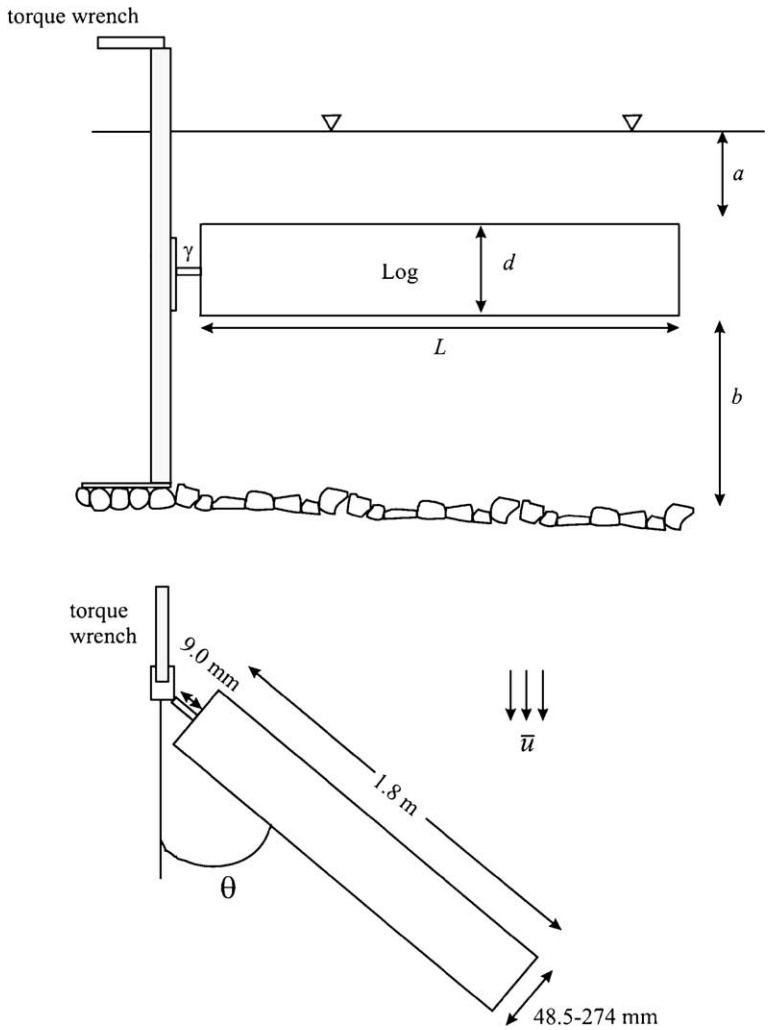

Fig. 1. Illustration of measurement apparatus used to measure torque on PVC "logs". (a) Apparatus geometry within the stream channel. (b) The angle θ and log dimensions.

where T is the torque. We used Eq. (2) to calculate F_d from torque measurements and then used Eq. (1) to calculate C_D^{app}.

4. Results and discussion

Here we present and interpret our field measurements and compare them with published lab measurements (e.g., Gippel et al., 1996). For the range of Re in the two rivers, and typical of most large woody debris in natural settings, the drag coefficient for a circular cylinder (C_D) in an infinitely large volume of fluid is between about 1.0 and 1.2 (e.g., Batchelor, 1967). Drag coefficients in our experiments were thus expected to be essentially independent of Re, and we could focus on geometric properties of woody debris. A detailed summary of all measurements and measurement conditions is compiled in a thesis (Hygelund, 2002).

4.1. Effects of orientation

The curve in Fig. 2 shows the relationship between torque and log orientation, θ, that would be predicted

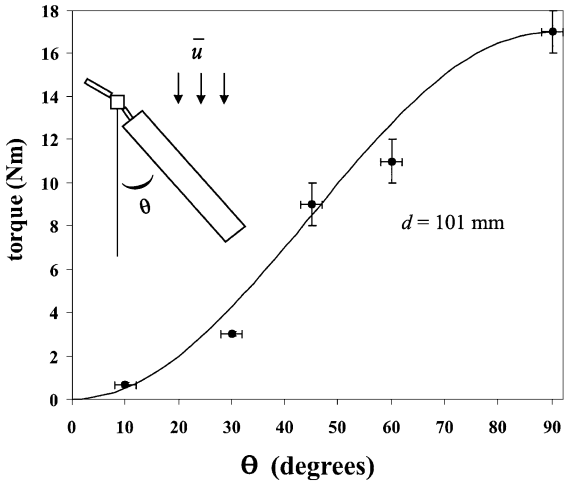

Fig. 2. Relationship between torque and the orientation of a log. Example shows measurements for the 101-mm diameter log in the Fall River. The curve defines the relationship that would be predicted if torque was independent of orientation.

if C_D^{app} is independent of orientation. θ is defined such that it is 0° if the log is aligned parallel to the flow, and 90° if it is aligned perpendicular to the flow (see Fig. 1). Generally, our data show a relationship similar to that expected if C_D^{app} is independent of orientation, although the uncertainty in C_D^{app} becomes large for small θ due to the approximately 5° uncertainty in determining θ in a field setting.

Our findings differ from the flume measurements reported in Fig. 2 of Gippel et al. (1996). Their results are similar to ours for θ between about 50° and 90°. Gippel et al. (1996), however, found an observable decrease of C_D^{app} for smaller angles (though as θ approaches 0°, C_D^{app} again approaches its value for θ>50°). The nearly constant C_D^{app} for large (and very small) θ can be explained by the log acting as a bluff body such that the water is forced either directly over or under the log. For more angled logs, there is a component of flow that develops parallel to the log that appears to reduce C_D^{app} in the flume experiments. The reason for our nearly constant C_D^{app} is not obvious. The most significant difference between the two sets of experiments is the rough bed in our field measurements that results in a vertical variation of velocity. We thus hypothesize that for the case of angled logs, the vertical gradient in velocity results in a larger component of fluid acceleration under the log (rather than parallel to the log) so that angled logs continue to resemble bluff bodies.

4.2. Effects of depth

Fig. 3 shows how C_D^{app} varies with a quantity we term as the depth ratio. The depth ratio is defined as the height of the water below the log divided by the height of the water below the log (b) divided by sum of the heights above and below log (a+b). In Fig. 3a, C_D^{app} is calculated with the depth-averaged velocity; in Fig. 3b, C_D^{app} is calculated using a local velocity and denoted C_{Dl}^{app}. For the 48.5-mm diameter log, C_D^{app} increases by a factor of 2.5 as the depth ratio increases from 0.2 to 1.0. This effect becomes less apparent for the larger diameter logs, and C_D^{app} varies negligibly with the depth ratio for the 168-mm and greater diameter logs. These findings indicate that to a good approximation, the drag does not vary with depth for logs with diameters greater than about one-third of the channel depth.

The relationship between C_D^{app} and depth for the smaller diameter logs essentially disappears when it is recalculated with the local velocity (C_{Dl}^{app}). These results suggest that larger diameter logs are wide enough that the velocity they "feel" is more similar to the depth-averaged velocity than any particular point of local velocity (see Fig. 4). However, the smaller logs have small enough diameters that the local velocity rather than a depth-averaged velocity will most greatly affect the drag.

The drag coefficients based on the local velocity for small cylinders are larger than the classical values based on measurements made on circular cylinders in air (see, e.g., Batchelor, 1967) or in towing tank experiments in water (Gippel et al., 1996). Our larger values may reflect a combination of the unsteady nature of natural stream flow and additional "induced drag" created by the interactions between the wake behind the log, the water surface, and the rough streambed. The so-called induced drag is created by vortices that develop downstream of the log (Batchelor, 1967, p. 331).

In the flume experiments reported by Gippel et al. (1996), velocity did not vary with depth and, unless the log was very close to the bottom, C_D^{app} did not vary significantly with depth. Fig. 3, however, shows

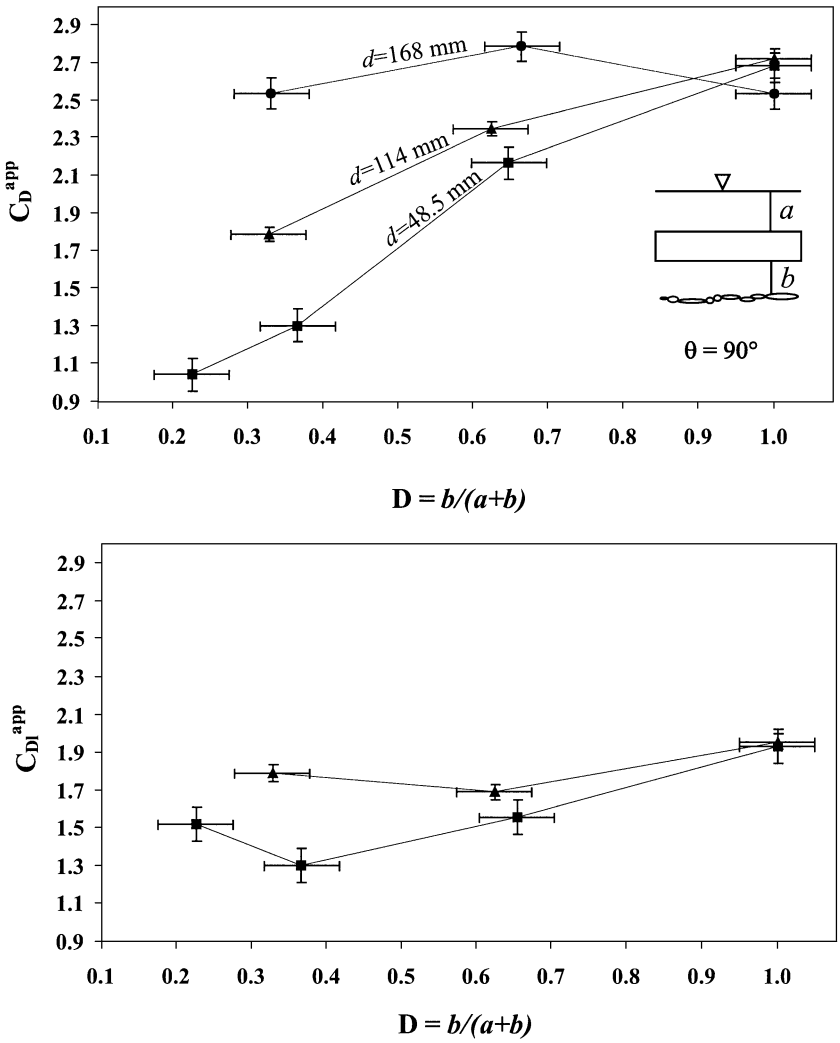

Fig. 3. (a) Relationship between the apparent drag coefficient C_D^{app} and a depth ratio $D=b/(a+b)$ as illustrated in the inset. $\theta=90°$ (measurements made in the Quinn River). (b) C_D^{app} calculated with the local velocity C_{Dl}^{app}.

that a depth dependence of C_D^{app} should be expected for "small" logs in natural streams owing to the depth dependence of velocity. Consequently, placing logs on the bottom of gravel bedded stream will not have substantial impact on channel roughness. By contrast, Gippel et al. (1996) also found that C_D^{app} increased when logs were placed very near the stream bottom due to a region of nearly stagnant water created upstream of the log. In a stream with a rough bottom, water can continue to flow under the log (and through the gravel on the stream bottom), explaining why C_D^{app} does not appear to increase in our measurements.

4.3. Effects of blockage

C_D^{app} may also depend on the ratio of the area obstructed by the log in the river to the cross-sectional flow area. This quantity is called the blockage B, where $B=d/\bar{z}$, d is the submerged log diameter, and $\bar{z}$ is the depth of the water (Ranga Raju et

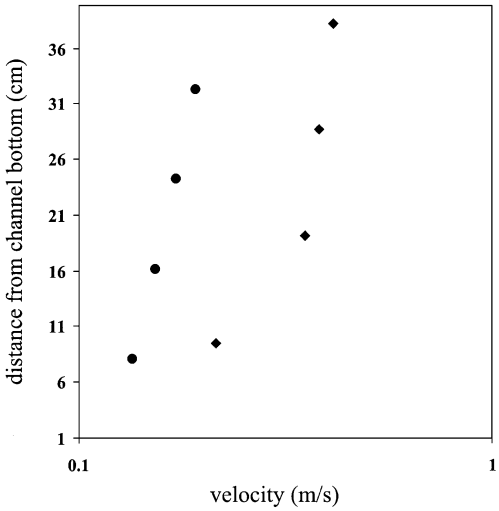

Fig. 4. Log-linear graph showing velocity vs. depth for the Fall River (diamonds) and the Quinn River (circles).

al., 1983; Shields and Gippel, 1995). Gippel et al. (1992) performed a series of towing tank and flume experiments, for which Shields and Gippel (1995) propose that the relationship between drag and blockage can be expressed as

$$C_D^{app} \approx \frac{C_D}{(1-B)^2}. \quad (3)$$

C_D is the drag coefficient for the cylinder in an infinitely large volume of fluid, and for $10^3 < Re < 10^5$, C_D has been experimentally determined to be approximately between 1.0 and 1.2 (Batchelor, 1967). Conservation of mass requires that the velocity per unit area upstream, $\bar{u}$, is equal to the velocity per unit area that is diverted around the log, U. Thus, the velocity increase will be $U = \bar{u}/(1-(d/\bar{z}))$, which is equal to $U = \bar{u}/(1-B)$. Thus, because drag scales with velocity squared (Eq. (1)), C_D^{app} might be expected to scale with $1/(1\text{-}B)^2$.

In Fig. 5, we show our results along with a curve showing the predicted relationship between C_D^{app} and B described by Eq. (3) of Shields and Gippel (1995). Shields and Gippel based their analysis of the relationship between C_D^{app} and B on a set of experiments where B ranged between 0.03 and 0.3. In our field measurements, B ranges up to 0.7. While the magnitude and scatter of our data is similar to the data presented in Shields and Gippel (for $B < 0.3$), Fig. 5 shows a poor correlation between C_D^{app} and B, especially for large B. Indeed, a Student's t-test analysis of the experimental data indicated that the null hypothesis (no relationship) cannot be rejected at the 95% confidence level.

The absence of a relationship between C_D^{app} and B suggests that the drag is dominated by the incoming (upstream) velocity of the water, rather than the maximum velocity of the water as it is accelerated around the log. For the Reynolds numbers typical of large woody debris, drag will be dominated by normal stresses acting on the log (i.e., friction drag is relatively insignificant). Because the flow will separate as it moves around the edge of bluff bodies, such as logs, the pressure on the downstream side of the log will be approximately constant. On the forward face of the log, from Bernoulli's theorem, the pressure will be proportional to the velocity of the incoming fluid squared. The drag will thus scale with the upstream velocity squared. Alternatively, the lower-than-predicted values of C_D^{app} at large B may be caused by an interaction between the flow and the streambed that will affect flow near the log and in the wake behind the log—changing the induced drag (see Section 4.2). Our measurements were conducted in gravel-bedded streams where the bed surfaces were rough and the log diameters were not orders of magnitude different from the mean size of the bed material (d_{50} ranged between 18 and 40 mm).

4.4. Effects of branches

We added 30, 254 mm long and 25 mm wide, pegs to the 168-mm diameter log to determine if increasing the roughness of its surface (adding leafless branches) had an effect on the drag. Overall, the same amount of torque (to within measurement uncertainty) was exerted on the smooth surface as was exerted on the same log with branches under the same experimental conditions. Gippel et al. (1996) performed similar experiments, also comparing apparent drag coefficients for cylinders with those for cylinders plus model branches, and they reported similar results.

By adding branches, we increased the surface area of the log; thus, we might expect the torque to

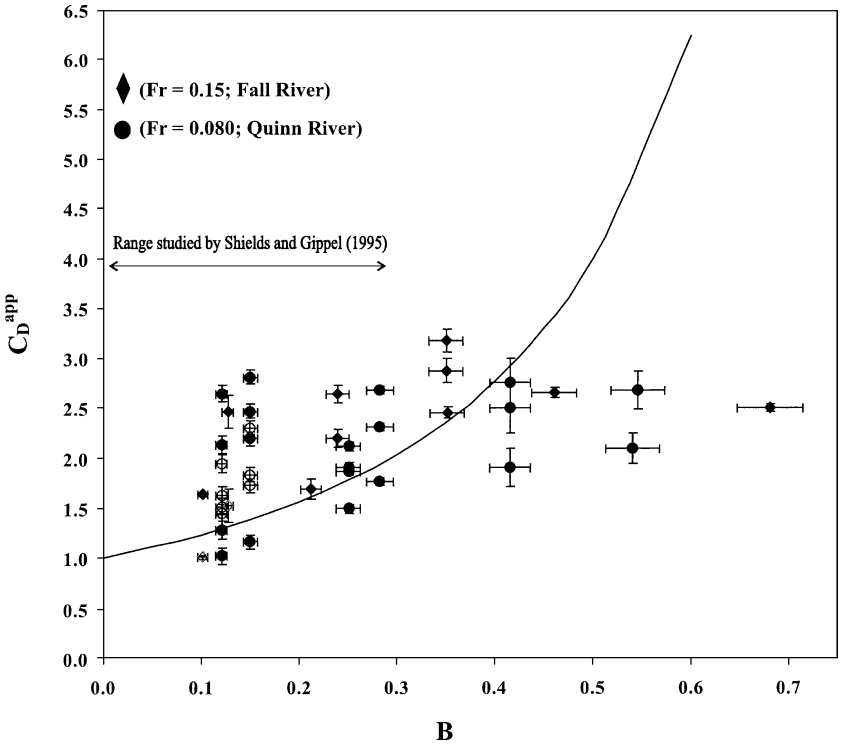

Fig. 5. Relationship between C_D^{app} and blockage B. Circles: Quinn River; diamonds: Fall River. Filled symbols represent C_D^{app} calculated with the depth-average velocity, and open symbols represent C_D^{app} calculated with the local velocity. The curve shows the experimentally determined relationship between C_D^{app} and B by Shields and Gippel (1995) for $B < 0.3$. For blockages less than about 0.3, the depth of the log in the water affects the relationship between C_D^{app} and B (see Fig. 3). The magnitude and scatter between C_D^{app} and B are compatible with the data in Shields and Gippel (1995). However, at larger blockages, no relationship is apparent between C_D^{app} and B, and $C_D^{app} \approx 2.1$.

increase. The branches, however, caused the approaching flow to separate and generated turbulence in the flow impinging on the log. Because the area A in Eq. (1) increased and the drag force F_d did not change, then C_D^{app} actually decreased.

5. Summary

The goal of the present study was to characterize some of the hydraulic effects of woody debris in streams. To conclude, we briefly illustrate how the measurements may be applied to fluvial systems and be used to interpret field measurements. As a specific example, we will consider the Cultus River in central Oregon, USA, a spring-fed river that has a nearly constant discharge (Manga, 1997). As we can see in Fig. 6, the Cultus River contains many large pieces of wood (mostly windblown lodgepole pine), with typical diameters of 20 cm. The mean separation of the logs is about 60 times their diameter so that the hydrodynamic interactions between logs due to wake interference can be neglected.

The wood in the Cultus is visually distinctive. What are the reach-averaged hydraulic effects of this wood? One convenient way of characterizing the effect of woody debris is through a stress partitioning equation, in which we estimate the flow resistance provided by the wood. The total channel shear stress, τ_0, is the weight of the water in the downstream direction per unit area of the bed

$$\tau_0 = \rho g R s \tag{4}$$

Fig. 6. Photograph of the Cultus River, central Oregon, USA. Note the person in the center of the photograph for scale. Owing to the nearly constant discharge in this river (Manga, 1997), the wood is very stable.

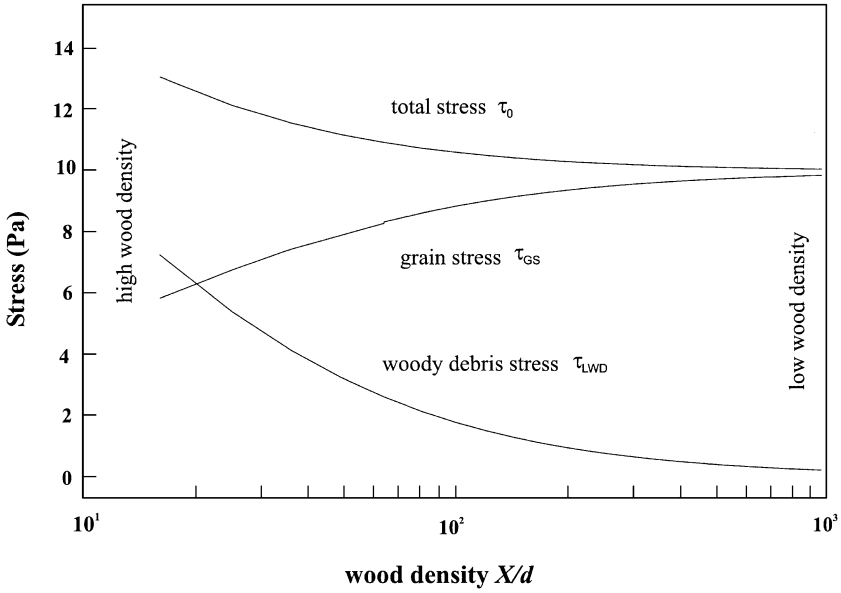

Fig. 7. Relationship between debris spacing X/d (X is the distance between logs and d is the log diameter), the total stress τ_0, the grain stress, τ_{GS}, and the woody debris stress, τ_{LWD} for the Cultus River. In these calculations, we used field-determined values of mean slope ($s = 0.0035$), mean water depth ($\bar{z} = 0.36$ m), water velocity ($\bar{u} = 0.36$ m/s), $X/d = 60$, and $C_D^{app} = 2$.

where R is the hydraulic radius and s is the slope of the energy gradient. Because Fr is small in the Cultus River, s will be close to the water surface slope. Assuming steady, uniform flow, τ_0 can be partitioned between various components, each of which characterizes a particular roughness element. We will assume for simplicity here that there are only two sources of roughness in the Cultus River: wood and bed roughness. We can thus write

$$\tau_0 = \tau_{GS} + \tau_{LWD} \tag{5}$$

where τ_{GS} characterizes the bed roughness and τ_{LWD} is the stress borne by woody debris. τ_{LWD} can be calculated by dividing the drag force acting on woody debris, Eq. (1), by the area of the bed the debris covers (e.g., Robert, 1997). A force balance for these components can be written as (e.g., Nepf, 1999)

$$\underset{\tau_0}{\underset{\downarrow}{\rho g \bar{z} s_b}} = \underset{\tau_{GS}}{\underset{\downarrow}{\rho C_B \bar{u}^2}} + \underset{\tau_{LWD}}{\underset{\downarrow}{\rho C_D^{app} \frac{d}{2X} \bar{u}^2}} \tag{6}$$

where C_B is a drag coefficient for the bed and X is the distance between logs. Following Manga and Kirchner (2000), we can now solve Eq. (6) to determine the effect of wood density on stress partitioning, subject to the assumptions that the discharge, channel width, slope, and size of bed materials do not change. Fig. 7 shows the different components of stress and total stress as a function of wood density. Fig. 7 shows two of the significant features of wood in rivers. First, as the density of wood increases, the total stress increases because the water depth increases (mean water depth is proportional to τ_0). Second, the fraction of stress borne by the bed decreases as the wood density increases. The results shown in Fig. 7 are examples of hydraulic processes with geomorphic implications that explicitly require knowledge of the drag coefficients we determined in this study.

In summary, our direct measurements of the torque required to hold circular cylinders at different depths and orientations allow us to calculate the effect of geometric properties on C_D^{app} in natural stream settings. These results contribute new information about the effects of a rough bottom on the roughness provided by wood in rivers and add to previous experimental work conducted by Gippel et al. (1996). Our results suggest that the orientation and depth of a log in a river have small effects on C_D^{app}, although the local velocity becomes important for calculating C_D^{app} for logs with diameters that are small relative to the water depth. We find that the effect of blockage (B), the ratio between the depth obstructed by the log and the water depth, is consistent with the experimental findings of Gippel et al. (1996) for small blockages ($B < 0.3$), but have no measurable effect on C_D^{app} at larger blockages. We also assessed how adding branches to a log affected C_D^{app}. We found that the drag force did not change when leafless branches were added, even though the surface area of the log was increased, implying that C_D^{app} decreased.

In our study, not all effects could be assessed. In particular, we did not account for effects caused by bedforms that may be created by the addition of wood to the channel. Nevertheless, our measurements provide improved estimates of C_D that can be incorporated into models that require knowledge of the drag on woody debris, such as those predicting the threshold for wood mobility (e.g., Braudrick and Grant, 2000), wood stability (e.g., D'Aoust and Millar, 2000), and stress partitioning (Buffington and Montgomery, 1999; Manga and Kirchner, 2000).

Acknowledgements

This work was supported by NSF EAR-9701768. D. Senkovich and N. Schaeffer provide technical help, and we thank R. Millar and C. Gippel for constructive suggestions.

References

Abbe, T.B., Montgomery, D.R., 1996. Large woody debris jams, channel hydraulics and habitat formation in large rivers. Regulated Rivers: Research and Management 12, 201–221.

Assani, A.A., Petit, F., 1995. Log-jam effects and bed-load mobility from experiments conducted in a small gravel-bed forest ditch. Catena 25, 117–126.

Batchelor, G.K., 1967. An Introduction to Fluid Dynamics. Cambridge Univ. Press, New York.

Bilby, R.E., 1983. Removal of woody debris may affect stream channel stability. Journal of Forestry 82, 609–613.

Bilby, R.E., Ward, J.W., 1991. Characteristics and function of large woody debris in streams draining old-growth, clear-cut, and second-growth forest in southwestern Washington. Canadian Journal of Aquatic Science 48, 2499–2508.

Bisson, P.A., Bilby, R.E., Bryant, M.D., Dolloff, C.A., Grette, G.B., House, R.A., Murphy, M.L., Konn, K.V., Sedell, J.R., 1987. Large woody debris in forested streams in the Pacific northwest: past, present and future. In: Salo, E.O., Cundy, T.W. (Eds.), Streamside Management: Forestry and Fishery Interactions. College of Forest Resources, University of Washington, Seattle, pp. 143–190.

Braudrick, C.A., Grant, G.E., 2000. When do logs move in rivers? Water Resources Research 36, 571–583.

Braudrick, C.A., Grant, G.E., Ishikawa, Y., Ikeda, H., 1997. Dynamics of wood transport in streams: a flume experiment. Earth Surface Processes and Landforms 22, 669–683.

Buffington, J.M., Montgomery, D.R., 1999. Effects of hydraulic roughness on surface textures of gravel-bed rivers. Water Resources Research 35, 3507–3521.

D'Aoust, S.G., Millar, R.G., 2000. Stability of ballasted woody debris habitat structures. Journal of Hydraulic Engineering 126, 810–817.

Dudley, S.J., Fischenich, J.C., Abt, S.R., 1998. Effects of woody debris entrapment on flow resistance. Journal of the American Water Resources Association 34, 1189–1197.

Gippel, C.J., O'Neill, I.C., Finlayson, B.L., 1992. The Hydraulic Basis of Snag Management. Centre for Environmental Applied Hydrology, Department of Civil and Agricultural Engineering, University of Melbourne, Victoria, Australia. 116 pp.

Gippel, C.J., O'Neill, I.C., Finlayson, B.L., Schnatz, I., 1996. Hydraulic guidelines for the reintroduction and management of large woody debris in lowland rivers. Regulated Rivers: Research and Management 12, 223–236.

Hygelund, B.N., 2002. Geomorphic and hydraulic effects of large woody debris: insights from spring-dominated streams in the Oregon Cascades. MS Thesis, University of Oregon, Eugene, 70 pp.

Lisle, T.E., 1995. Effects of coarse woody debris and its removal on a channel affected by the 1980 eruption of Mount St. Helens, Washington. Water Resources Research 33, 1813–1822.

Manga, M., 1997. A model for discharge in spring-dominated streams, and implications for the transmissivity and recharge of quaternary volcanics in the Oregon Cascades. Water Resources Research 33, 1813–1822.

Manga, M., Kirchner, J.W., 2000. Stress partitioning in streams by large woody debris. Water Resources Research 36, 2373–2379.

Nakamura, F., Swanson, F.J., 1993. Effects of coarse woody debris on morphology and sediment storage of a mountain stream in western Oregon. Earth Surface Processes and Landforms 18, 43–61.

Nepf, H.M., 1999. Drag, turbulence, and diffusion in flow through emergent vegetation. Water Resources Research 35, 479–489.

Piegay, H., Gurnell, A.M., 1997. Large woody debris and river geomorphological pattern: examples from SE France and S. England. Geomorphology 19, 99–116.

Ranga Raju, K.F., Rana, O.P.S., Asawa, G.L., Pillai, A.S.N., 1983. Rational assessment of blockage effect in channel flow past smooth circular cylinders. Journal of Hydraulic Research 21, 289–302.

Robert, A., 1997. Characteristics of velocity profiles along riffle-pool sequences and estimates of bed shear stresses. Geomorphology 19, 89–98.

Robison, E.G., Beschta, R.L., 1990. Coarse woody debris and channel morphology interactions for undisturbed streams in southeast Alaska, USA. Earth Surficial Processes and Landforms 15, 149–156.

Shields, F.D., Gippel, C.J., 1995. Prediction of effects of woody debris removal on flow resistance. Journal of Hydraulic Engineering 121, 341–354.

Smith, R.D., Sidle, R.C., Porter, P.E., Noel, F.R., 1993. Effects of experimental removal of woody debris on the channel morphology of a forest, gravel-bed stream. Journal of Hydrology 152, 153–178.

Trimble, S.W., 1997. Stream channel erosion and change resulting from riparian forest. Geology 25, 467–469.

Whiting, P.J., Moog, D.B., 2001. The geometric, sedimentologic and hydrologic attributes of spring-dominated channels. Geomorphology 92, 149–156.

Whiting, P.J., Stamm, J., 1995. The hydrology and form of spring-dominated channels. Geomorphology 12, 233–240.